

Opportunistic spectral access through suppression of impulsive interference

Accès spectral opportuniste par suppression de l'interférence impulsive

Jeebak Mitra and Lutz Lampe*

Cognitive radios are slated to be the next generation of smart transceivers that can opportunistically access spectrum through dynamic sensing of their immediate radio frequency (RF) environment. Such spectral sharing will be limited primarily by the interference that a cognitive user may potentially cause to the licensed primary user of the band. In particular, all cognitive transmitters located within a certain region of interference of a primary user will have to refrain from transmitting data. Given that most cognitive users will need to transmit data only intermittently and that there will be only a finite number of such users in the RF neighbourhood of a primary user, it is conceivable that the resulting interference at the primary will be more structured than can be described by a white Gaussian noise model. This opens the door for interference mitigation techniques that exploit the interference structure. In this work, methods to mitigate the effects of potentially harmful interference caused by active secondary users through intelligent signal processing at the receiver of the primary user are investigated, such that the perimeter of the region of interference can be reduced, creating greater opportunities for the secondary users while meeting interference constraints. Receiver structures for the more practical scenario of temporally correlated interference are introduced, and the achievable gains when applying simple yet effective interference suppression methods are quantified.

Des radios cognitives sont prévues pour être la prochaine génération d'émetteurs-récepteurs à puce, qui seront capables d'une façon opportuniste d'avoir accès au spectre par la détection dynamique de leur environnement de fréquence radio (RF) immédiat. Un tel partage spectral sera limité principalement par l'interférence qu'un utilisateur cognitif peut potentiellement causer à l'utilisateur primaire autorisé de la bande. En particulier, tous les émetteurs cognitifs placés dans une certaine région d'interférence d'un utilisateur primaire devront s'abstenir de la transmission de données. Étant donné que la plupart des utilisateurs cognitifs devront transmettre des données seulement par intermittence et qu'il y aura seulement un nombre limité de ces utilisateurs dans le voisinage RF d'un utilisateur primaire, il est imaginable que l'interférence résultante au primaire sera plus structurée qu'elle peut être décrite par un modèle blanc de bruit sonore Gaussien. Cela ouvre la voie à des techniques d'atténuation du brouillage qui exploitent la structure d'interférence. Dans ce travail, les méthodes pour atténuer les effets d'interférence potentiellement nuisible causée par des utilisateurs secondaires actifs par le traitement intelligent de signal au niveau du récepteur de l'utilisateur primaire sont examinées, tel que le périmètre de la région d'interférence peut être réduit, ce qui crée davantage de possibilités pour les utilisateurs secondaires tout en respectant des contraintes d'interférence. Les structures des récepteurs pour le scénario plus pratique d'interférence temporellement corrélée sont introduites, et les gains réalisables en raison des méthodes simples mais efficaces de suppression des interférences sont quantifiés.

Keywords: impulsive interference; interference suppression; spectrum sharing

I Introduction

The traditional approach based on licensed use of spectral resources has led to radio frequency spectrum being increasingly scarce, and hence it was natural to question how well the allocated spectrum was being used. The findings of the Spectrum Policy Task Force [1], although a surprise to many, established that, depending on the population density of a region, most spectral bands tend to be vastly underutilized [2]. This conclusion makes a strong case for pursuing more efficient use of the available spectrum by allowing *unlicensed* users to operate in unused spectral regions when it can be ensured that the (licensed) primary user of that band does not face harmful interference due to the (unlicensed) secondary¹ users. Although this idea has opened up a huge window of opportunity for the beyond-third generation (3G) wireless scenario, namely, the realm of cognitive radio (CR), the technical challenges that must be overcome to ensure an amiable coexistence of primary and secondary users are formidable [3]–[4].

The first and foremost task in order for secondary users to be able to make use of the unutilized spectrum is to sense the band of interest and ensure that it is not being used by a primary user. In CR terminology this is referred to as radio scene analysis (RSA) [3]. Using the information gathered through RSA, a conventional cognitive user obeys the following dictum: initiate transmission if and only if the band is sensed to be free [3]. Depending on whether the secondary user is multi-band or not, it will either hop to a different frequency band and repeat the RSA operation or it will continue to sense the same band until it is free before it eventually transmits. Thus the basic premise of cognitive radio is the ability to sense the surrounding RF environment and then react accordingly.

Since interference is the single most important limiting factor that prevents a secondary user from using available spectrum, it is imperative to define what constitutes *harmful* interference for a primary user. The two metrics that are typically used to sense the level of interference [5] in the band of interest are the signal-to-(interference + noise) ratio (SINR), which entails a data-aided (pilot symbols) or blind estimation of both the wanted and unwanted signal powers, and a relatively newly coined metric known as interference temperature (IT) [1], [3], which can be quite easily measured at the receiver by collecting the RF power in a given frequency band when no useful information is being received. The latter metric allows CR to deviate from the traditional practice of imposing transmit power limits and permits a receiver-centric perspective in determining the feasibility of transmission for a secondary user. More specifically, the proponents of the IT-based approach argue that simultaneous transmission by sec-

*Jeebak Mitra and Lutz Lampe are with the Department of Electrical and Computer Engineering, University of British Columbia, 5500 – 2332 Main Mall, Vancouver, British Columbia V6T 1Z4, Canada. E-mail: {jeebakm, lampe}@ece.ubc.ca. This paper was awarded a prize in the Student Paper Competition at the 2009 Canadian Conference on Electrical and Computer Engineering. It is presented here in a revised format.

¹Throughout the paper the terms *secondary* and *cognitive* are used interchangeably to denote the unlicensed users of a frequency band.

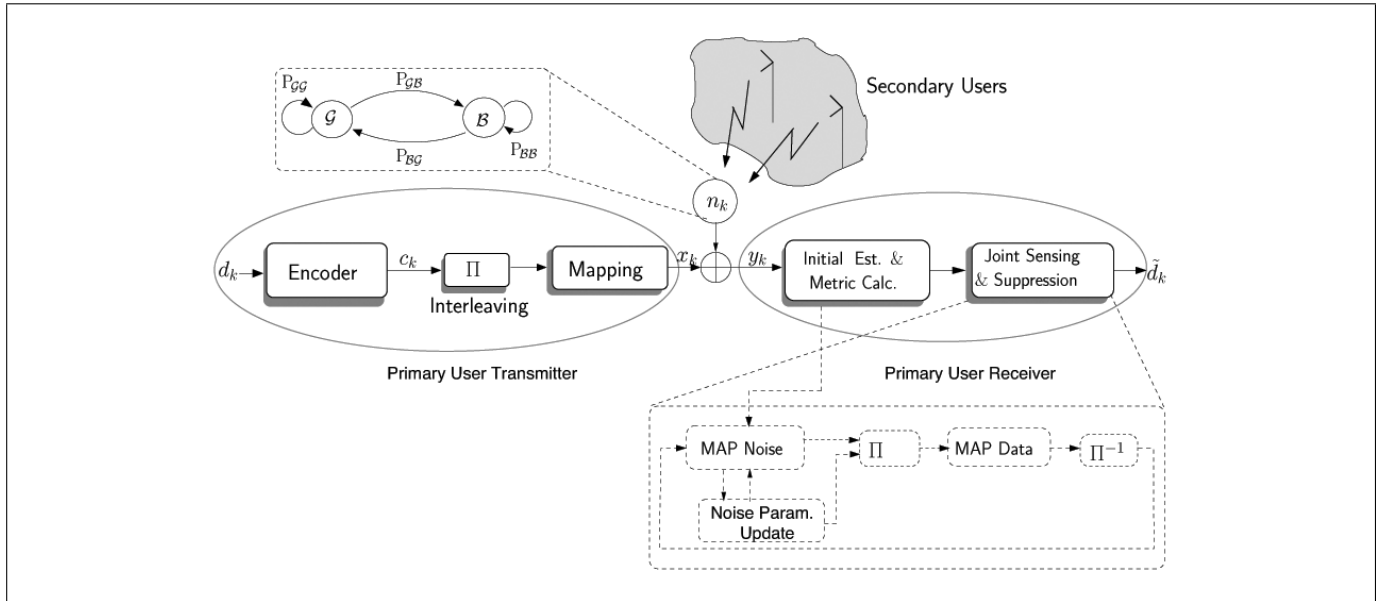


Figure 1: System model for the overall transmission and reception modules. The Joint Sensing and Suppression block forms the core of the receiver, where the MAP Noise module uses the inherent memory of the non-interleaved received sequence to estimate the noise states while data detection is carried out on the interleaved symbols by MAP Data.

secondary users may very well be permitted as long as the noise floor at a licensed user can be maintained below an acceptable IT upper limit [1], [3], [5]–[6]. In this way, a higher utilization of the spectrum can potentially be achieved. While this is a passive approach that could be more aptly labelled as interference tolerance, a more effective approach would be to actively mitigate the unknown interference at the primary user, thus permitting a much higher cap on the instantaneous interference temperature. The latter approach will be the focus of the work presented here. It offers multiple advantages, including higher throughput and reduction of the so-called *region of interference* for the primary user [7]. The idea is to take a more active approach to opportunistic spectral access by creating more opportunities for unlicensed users to transmit data through improved protection for the primary users of a given frequency band. This in effect increases the sum capacity of the system [8]. However, the proposed approach does not go as far as recently advocated information theoretic techniques [9] that assume the availability of the codebook of the interference signals in a non-causal fashion and call for substantial coordination among the various users.

It can be noted that sensing a cognitive user's RF environment to ensure minimal additional interference to the primary user when it is active is a fairly challenging problem, and the current state of the art cannot guarantee detection of a primary signal transmission in all situations [4], [10]–[11]. Hence, in a CR environment one can expect interference at the primary receiver in addition to the Gaussian thermal noise, $\mathcal{N}(0, \sigma_G^2)$, that is typically considered to impair the received signal in conventional communication systems. The same holds true for secondary receivers since, although a secondary transmitter would sense its RF environment before transmitting, the corresponding receiver may be susceptible to co-channel interference from other secondary users in its vicinity unless an elaborate centralized access scheme is deployed [12].

Furthermore, secondary traffic is expected to be intermittent. This characteristic, combined with the technical specifications of next-generation wireless systems (e.g., frequency hopping in a multi-band orthogonal frequency-division multiplexing (MB-OFDM) system), will cause the interference in a frequency band of interest to be more structured than can be described using a Gaussian distribution alone [3], [7], [13]. Such non-Gaussian behaviour can lead to considerable performance degradation when conventional matched filtering techniques are used at the receiver [14]. In the literature, a mixture of two Gaussians with variances σ_B^2 and σ_G^2 such that $\sigma_B^2 \gg \sigma_G^2$, along with a mixing parameter $0 \leq \epsilon \leq 1$ whose physical interpretation is

the probability of occurrence of the interference, has been frequently used to model an impulsive interference process [15]–[16]. However, an implicit assumption often made in using this model is the temporal independence of the interfering signals. In most RF environments, this will not be true since, if a certain interferer is active during the current time slot, the probability that it will be active in the next time slot is very high [17], making temporal dependence imminent.

In this paper, a probabilistic approach is used to model the correlated interference plus noise at the primary receiver as a Markovian process, leading to parameterization of the unknown interference. An active interference mitigation technique is then adopted in tandem with energy detection (ED)–based sensing at the receiver of the primary user to reduce its perceived level of interference. In particular, the temporal dependence of the interference process is exploited to alleviate its adverse effects on the received signal, and novel semi-blind and blind techniques are devised to estimate the instantaneous interference levels. Applying well-known tools from the domain of decoding in correlated noise environments [18]–[20], an iterative maximum *a posteriori* (MAP) decoder for a convolutionally coded system is developed that, in conjunction with the proposed interference estimation techniques, exhibits substantial performance improvements in the presence of interfering signals. The active mitigation of the presumably harmful interference at the primary receiver benefits the overall CR system by pushing the permissible IT limit much higher than the allowable noise floor with conventional receivers. The efficacy of these approaches is manifested by a comparison with standard decoding techniques.

The rest of the paper is organized as follows. Section II describes the system model used and also the specifics of the interference modelling. The central focus of this paper is a joint sensing and suppression algorithm explained in detail in Section III, followed by a brief description of the conventional and an idealized detection approach in Section IV. Section V presents numerical results to demonstrate the capabilities of interference mitigation algorithms. Finally, relevant conclusions are provided in Section VI.

II System model

In this section, the transmission system is introduced, and details of the model used to represent the interference caused by simultaneous transmissions or other spurious impairing signals in the RF neighbourhood

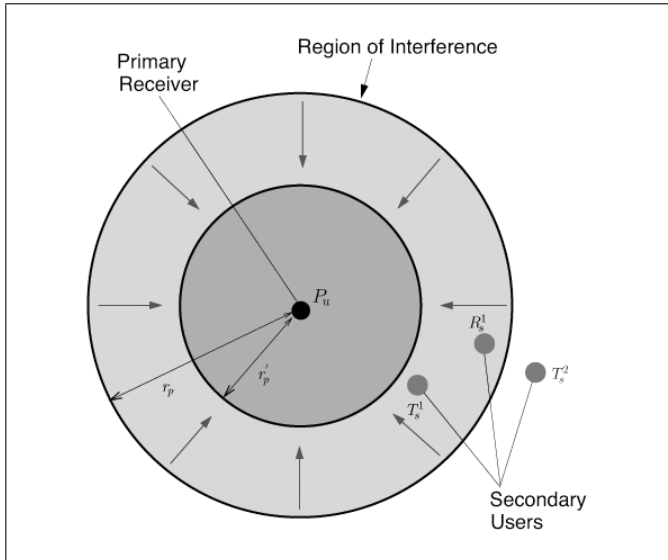


Figure 2: Typical interference scenario for a cognitive transmission environment with multiple secondary users that are expected to transmit only when there is no harmful interference to the primary user, P_u . The circle with radius r_p denotes the region of interference for P_u in which transmission by cognitive users may result in harmful interference. Reduction of r_p to r'_p permits users such as T_s^1 and R_s^1 to communicate.

of the desired primary receiver are presented. Fig. 1 presents a block diagram of the essential transmitter and receiver units and the channel model. Usually all primary receivers are equipped with the requisite circuitry to sense the radio environment, although this has heretofore been used only for channel estimation. Here the additional use of the primary user's sensing abilities during reception of user data is proposed, along with an additional comparator block at the RF front-end of the primary receiver to act as a decision device. This is somewhat akin to RSA, which has been associated only with the cognitive user in CR systems [3]. The end goal of such a sensing exercise at the primary user would, however, be different from that at a secondary. In the proposed communication framework, the functional use of the primary's sensing abilities is to determine whether a received symbol is impaired by interference. For now the focus will be on the rest of the receiver blocks in Fig. 1, and a discussion of the details of the interference estimation through sensing is postponed until Section III.

The primary user's message is composed of information bits $d_k \in \{0, 1\}$, emitted by a source with uniform probability, that are subsequently encoded by an encoder to produce coded bits c_k . It should be noted that encoding is crucial to enable a primary user to mitigate interference from CRs. As can be seen in Fig. 1, an interleaver is used to reduce the effects of contiguous bits in error, and the interleaved symbols are then mapped to binary phase-shift-keyed (BPSK) symbols by the mapper to generate transmit symbols $x_k \in \{-1, 1\}$. When performance results are discussed in Section V, interleavers with both finite and infinite interleaving depth (ILD) will be considered. The transmitted BPSK symbols (x_k) are received after being affected by thermal noise and interference, hereafter collectively referred to as noise, and the equivalent discrete-time representation of the received symbol after filtering and Nyquist rate sampling is given by

$$y_k = \sqrt{E_s} x_k + n_k, \quad n_k = \begin{cases} w_k, & \text{no interference,} \\ w_k + i_k, & \text{with interference,} \end{cases} \quad (1)$$

where E_s is the energy of the received symbol and coherent detection is assumed. Furthermore, the primary-user channel is assumed to remain static for a number of codeword transmissions, and thus the effect of possible fading is included in E_s . The variable w_k represents self-generated thermal noise at the primary receiver, and i_k denotes the aggregate interference, a mathematical description of which is provided in the following. In Fig. 1, the Joint Sensing and Suppression (JSS)

block is of primary interest as it implements the algorithms to determine whether a received symbol is impaired by interference or not and accordingly applies a weighting factor to the decision metric for the corresponding symbol. The JSS block is based on an iterative exchange of soft information [21] between two blocks (MAP Noise and MAP Data in Fig. 1) using an instance of the forward-backward (FB) [22] algorithm, one each for noise and data estimation. In Section III it will be seen that the weight factor is in effect the instantaneous signal-to-noise power ratio (SNR) for the corresponding received symbol and hence that the JSS block also plays the role of a symbol-by-symbol SNR estimator. It should be noted that the JSS block is fundamentally different from SNR estimators for additive white Gaussian noise (AWGN) channels [23] since the noise distribution is non-homogeneous in the present case.

Interference model: The spatial distribution of the interferers is considered to be Poisson, which has frequently been used to model the geographical distribution of interferers in both cognitive [7], [24] and non-cognitive [13], [17] communication systems. Such a distribution implies that the number of interferers in a region \mathcal{R} is directly proportional to the area of the region, $\mathcal{A}_{\mathcal{R}}$. Furthermore, the probability distribution function (pdf) of interference with such a model, when $\mathcal{A}_{\mathcal{R}}$ is a circular region around the primary user (refer to Fig. 2), indicates that the distribution function is primarily governed by a few dominant interferers close to the receiver and thus has much heavier tails than a Gaussian [7]. This RF neighbourhood of the primary user will be referred to as the region of interference, which in Fig. 2 is the disc of radius r_p with P_u in the centre². Alternatively, the region of interference may also be defined as the minimum physical perimeter around the primary user that is regarded as the no-talk zone for a secondary user in order to meet the corresponding interference-temperature constraints. The mandate of cognitive radios [3], [7] dictates that transmission from, say, secondary transmitter T_s^1 to a secondary receiver R_s^1 , as depicted in Fig. 2, concurrently and in the same band as primary user P_u , may be allowed only if T_s^1 is outside P_u 's region of interference. The objective here is to reduce the region of interference for a given primary user from a circle of radius r_p to, say, r'_p , where $r'_p < r_p$ (see Fig. 2), by making the receivers more tolerant to the evidently non-Gaussian interference and thereby raising the cap on IT.

The above communication scenario dictates that the received signal at P_u is impaired by a superposition of signals from all potential interferers in a given time slot. As mentioned in Section I, it is stipulated that the non-Gaussian distribution of such interference at the primary receiver can be well modelled using a two-term Gaussian mixture distribution. It is further assumed that the temporal correlation of the interference, which can be attributed to both secondary traffic patterns and channel access techniques of the unlicensed users that give rise to non-overlapping dwell times in time and/or frequency, is modelled using a first-order Markov chain whose states are characterized by zero-mean conditionally Gaussian random variables with variances $\sigma_{\mathcal{G}}^2$ and $\sigma_{\mathcal{B}}^2$. The idea is to be able to model two different channel conditions, one of which occurs when no other user (primary or secondary) is using the channel and thus transmitted packets are affected only by the self-generated AWGN of the receiver. Since this state is favourable for transmissions, it is referred to as the good (\mathcal{G}) state. The component i_k in (1) models the cumulative interference with signal power, which is several times greater than can be modelled with the AWGN term w_k , creating the need for a higher-variance term for the so-called bad (\mathcal{B}) state. Let $s_k \in \{\mathcal{G}, \mathcal{B}\}$ be the state of the noise process at the k -th instant. Then by definition s_k is conditionally independent of the rest of the noise samples, given as s_{k-1} . The conditional distribution in a state $\mathcal{S} \in \{\mathcal{G}, \mathcal{B}\}$ is given by

$$p_{\mathcal{S}}(n_k) = p(n_k | s_k = \mathcal{S}) = \frac{1}{\pi \sigma_{\mathcal{S}}^2} \exp\left(-\frac{|n_k|^2}{\sigma_{\mathcal{S}}^2}\right). \quad (2)$$

²Note that the circular depiction of the region of interference in Fig. 2 is based on the assumption of an omni-directional antenna of the primary user. In general, due to physical phenomena such as shadowing and short-term fading, the actual region of interference will be an arbitrary polygon.

The variances σ_G^2 and σ_B^2 are used respectively to define the signal-to-thermal noise ratio, $\text{SNR} = E_s/\sigma_G^2$, and the signal-to-interference ratio, $\text{SIR} = E_s/\sigma_B^2$, of the overall system. The region of interference may thus be interpreted to be the region where the primary receiver can meet target performance criteria, e.g., bit error rate (BER), within a certain lower limit on the SIR. In (2), the evolution of n_k is governed by the transition probabilities $P_{S'S}$ from state S to state S' , where S and S' are in $\{\mathcal{G}, \mathcal{B}\}$. Since there are two states, there will be four sets of transitions that are governed by the respective transition probabilities depicted in the flow graph of Fig. 1. It is assumed that the Markov chain is irreducible and aperiodic and hence is completely specified by the transition probabilities $P_{\mathcal{G}\mathcal{B}}$ and $P_{\mathcal{B}\mathcal{G}}$, which in turn depend on the average duration in the states \mathcal{G} and \mathcal{B} respectively. This paper will focus specifically on the case where $P_{\mathcal{B}\mathcal{G}} \gg P_{\mathcal{G}\mathcal{B}}$, implying that the interference is intermittent.

III Joint sensing and suppression

Here the JSS approach is presented, which uses ED-based sensing at the receiver in conjunction with an expectation maximization (EM)-like [25] interference estimation that is shown to increase the tolerance of the intended receiver to spurious interference. Sensing at the primary user is carried out to determine the correct weighting factor applicable to the decoding metric of a received symbol, which is very different from the objective of spectrum sensing at the secondary, where it allows a secondary to gauge a transmission opportunity. RF sensing in itself relates to the classical binary hypothesis-testing problem where the null hypothesis (\mathcal{H}_0) represents the \mathcal{G} state and \mathcal{B} is the alternate hypothesis (\mathcal{H}_1) [4], [26]. The utility of JSS stems from more than just its hypothesis-testing abilities; in fact, it is concerned more with the processing applied to the information gleaned from the hypothesis-testing exercise. To obtain a thorough understanding of the estimation process, one needs to assume that varying levels of information are available at the receiver about the interference process.

In estimating the vector of transmitted symbols $\mathbf{x} = [x_1, \dots, x_N]$, where N is the block length, from the vector of received symbols $\mathbf{y} = [y_1, \dots, y_N]$, one is faced with the lack of knowledge of the interference parameters $\boldsymbol{\theta} = \{\sigma_G^2, \sigma_B^2, P_{\mathcal{B}\mathcal{G}}, P_{\mathcal{G}\mathcal{B}}, P(s_1 = \mathcal{G})\}$. The maximum-likelihood estimation of \mathbf{x} and \mathbf{s} is formulated along the lines of [18], where for a similar setting with interference by jamming, $\boldsymbol{\theta}$ is augmented by an auxiliary variable $\mathbf{P} = [P(x_1 = -1), \dots, P(x_N = -1)]$, representing the probability of \mathbf{x} on which the decisions about \mathbf{x} are eventually based, as

$$\begin{aligned} \hat{\boldsymbol{\theta}} &= \underset{\boldsymbol{\theta}}{\operatorname{argmax}}\{p(\mathbf{y}, \mathbf{x}, \mathbf{s} | \boldsymbol{\theta})\} \\ &= \underset{\boldsymbol{\theta}}{\operatorname{argmax}}\{p(\mathbf{y} | \boldsymbol{\theta}, \mathbf{x}, \mathbf{s})p(\mathbf{x} | \boldsymbol{\theta})p(\mathbf{s} | \boldsymbol{\theta})\}, \end{aligned} \quad (3)$$

where \mathbf{x} and $\mathbf{s} = [s_1, \dots, s_N]$ are the variables of interest that are to be determined by application of the EM approach [25]. As illustrated in Fig. 1 and also well outlined in [18], an EM approach naturally develops into an iterative estimation and decoding procedure for \mathbf{s} (MAP Noise) and \mathbf{x} (MAP Data), with the MAP Noise module augmented by a noise-parameter update. In the following, the modules for noise state estimation that builds on the Markovianity of the ambient noise and the MAP-based estimator for the transmitted bits which uses the code memory are presented.

III.A Interference state estimation

The MAP algorithm for the noise state estimation uses the received symbols \mathbf{y} together with the current parameter estimate $\boldsymbol{\theta}^{(n)}$ after n iterations. At the $(n+1)$ -th iteration, the probability of the transition $s_{k-1} \rightarrow s_k$ is given by [22]

$$\begin{aligned} \gamma^{(n+1)}(s_k, s_{k-1}) &= p^{(n)}(s_k | s_{k-1}) \\ &\times \sum_{\tilde{x}_k \in \{\pm 1\}} p^{(n)}(y_k | s_k, \tilde{x}_k)p^{(n)}(\tilde{x}_k), \end{aligned} \quad (4)$$

where $p^{(n)}(\tilde{x}_k)$ and $p^{(n)}(s_k | s_{k-1})$ are given by $\boldsymbol{\theta}^{(n)}$. All other relevant quantities of the MAP algorithm, such as the forward metrics $P(s_k | s_{k-1}, \mathbf{y}_1^k)$ and the backward metrics $P(s_k | s_{k+1}, \mathbf{y}_{k+1}^N)$ for the FB algorithm, can be computed using $\gamma(s_k, s_{k-1})$ to finally obtain the *a posteriori* probabilities (APPs) $p_{s_k}^{(n+1)}(S)$ of the noise states [18], [22]. The stationary transition probabilities of the Markov chain $P_{S_k S_{k-1}}$ can be determined from the joint probabilities of the noise states. For example, $P_{\mathcal{B}\mathcal{G}}$ is computed as

$$P_{\mathcal{B}\mathcal{G}}^{(n+1)} = \frac{\sum_{k=1}^N \nu_k(\mathcal{B}, \mathcal{G})}{\sum_{k=1}^N [\nu_k(\mathcal{G}, \mathcal{G}) + \nu_k(\mathcal{B}, \mathcal{G})]}, \quad (5)$$

where $\nu_k(A, B) = \gamma^{(n+1)}(A, B)$, $[A, B] \in \{\mathcal{G}, \mathcal{B}\}^2$. The maximization step of the EM algorithm also yields the expression for updating the variances of the noise process [18]. In particular, setting the derivative of $E\{\log(p(\mathbf{y} | \boldsymbol{\theta}, \mathbf{s}, \mathbf{x}) | \mathbf{y}, \boldsymbol{\theta}^{(n)})\}$ to zero yields the following new estimate:

$$(\hat{\sigma}_S^2)^{(n+1)} = \frac{\sum_{k=1}^N [(|y_k|^2 + E_s + 2\Re\{y_k^* s_k\})\Delta^{(n+1)}(x_k)p_{s_k}^{(n+1)}(S)]}{2 \sum_k p_{s_k}^{(n+1)}(S)}, \quad (6)$$

where $\Delta^{(n+1)}(x_k) = p^{(n+1)}(x_k = -1) - p^{(n+1)}(x_k = +1)$. The updated values of the variances and noise state APPs as obtained above are used by MAP Data as described below.

III.B MAP decoding for the code

An FB decoder similar in spirit to the one described above for the noise states is employed to determine the APPs of the information and the coded bits, where the states of the trellis are the states of the finite state machine (FSM) that describes the code.³ The received symbols and noise state APPs are de-interleaved and fed to the block denoted as MAP Data in Fig. 1. The branch transition probability $\Gamma(z_{k-1}, z_k)$, where z_k is the state of the FSM at the k -th instant, is computed using the following channel metric:

$$\lambda(\tilde{x}_k) = \sum_{S \in \{\mathcal{G}, \mathcal{B}\}} p(y_k | \tilde{x}_k, S)p_{s_k}^{(n+1)}(S)p^{(n)}(\tilde{x}_k), \quad (7)$$

where $p_{s_k}^{(n+1)}(S)$ is obtained from MAP Noise. Note that in (7), $p(y_k | \tilde{x}_k, S)p_{s_k}^{(n+1)}(S)$ is the implicit weighting, mentioned in Section II, as the Euclidean distance between y_k and \tilde{x}_k is weighted by $p_{s_k}^{(n+1)}(S)$, the probability of being in state S in the $(n+1)$ -th iteration, along with the corresponding variance estimate $(\hat{\sigma}_S^2)^{(n+1)}$. The metrics $\lambda(\tilde{x}_k)$ can be used to recursively compute the forward and backward metrics required to obtain the APPs $p^{(n+1)}(\tilde{x}_k)$, which are used in the next iteration of MAP Noise as components of $\boldsymbol{\theta}^{(n+1)}$.

III.C Initial estimation for noise variances

The successive refinement of the APPs of the noise states and the transmitted symbols through an exchange of soft information improves the performance of the JSS over iterations. For each iteration at the receiver, MAP Noise runs first so that MAP Data has a sufficiently good estimate of the noise state and the corresponding weighting factor. However, for the first iteration of MAP Noise, no information on $\boldsymbol{\theta}$ is available. Simulative evidence shows that while the initialization of the unknown Markovian probabilities to 0.5 does not affect the estimation process much (a result which is in agreement with the findings in [18]), the knowledge of the noise state variances is critical to successful decoding of the transmitted symbols. To this end, semi-blind and blind techniques are presented next to obtain initial estimates for the noise variances that help bootstrap the iterative estimation algorithm described above. The approaches presented below make use of a comparator (refer to Section II) that acts as a decision device following the

³Here a convolutional code is used, and thus a trellis-based approach is favourable. However, codes that are decoded by a factor graph, e.g., low-density parity check (LDPC) codes, are equally applicable.

RF sensing at the receiver. In particular, *outliers* are identified in the received symbol block in order to distinguish between desired and undesired RF signals. These methods are applicable to small block lengths and are bandwidth-efficient at the same time since no pilot symbols are used.

III.C.1 Semi-blind estimation

For semi-blind estimation, it is assumed that σ_G^2 is known at the receiver. However, no further knowledge regarding either the frequency or strength of the interfering signals is available. The rationale is that thermal noise is primarily attributed to device irregularities and hence can be measured off-line. The key sources of uncertainty in sensing the interference environment, therefore, are the other opportunistic (cognitive) transmitters in the region of interference of the desired user [7], [27]. Denoting the power of the k -th received symbol y_k as ψ_k , the semi-blind algorithm declares y_k as an outlier if ψ_k is greater than $\mathcal{T}_{\text{semi}}$, where $\mathcal{T}_{\text{semi}} = 5\sigma_G^2$. An initial estimate for σ_B^2 is obtained as [20]

$$\hat{\sigma}_B^2 = \sum_{y_k \in \mathcal{O}} \eta_k \left(\frac{|y_k + \sqrt{E_s}|^2 + |y_k - \sqrt{E_s}|^2}{2} \right), \quad (8)$$

where $\mathcal{O} = \{y_k : \psi_k > \mathcal{T}_{\text{semi}}, 1 \leq k \leq N\}$ and $\eta_k = \psi_k / \sum_{k \in \mathcal{O}} \psi_k$. Using a weighting factor η_k instead of equal weighting with, say, $1/|\mathcal{O}|$ ensures that an estimate $\hat{\sigma}_B^2$ is not overly skewed because of the presence of one or more strong interferers in a few time slots.

III.C.2 Blind estimation

Estimation for the case in which the receiver has absolutely no knowledge of the noise parameters and must obtain all the information it needs from the received data is now considered. Such a communication environment may very well occur when there are multiple cognitive nodes at a distance from the primary user that appear as weak Gaussian interference, in effect raising the noise floor beyond the device thermal noise, over a duration that is longer than that of the typical frame of the primary user, thus leading to an ambiguity regarding the value of σ_G^2 as well. As is obvious, this is a far more challenging task than the semi-blind approach described above. Two techniques are proposed here that use tools from the domain of robust statistics [28] to arrive at initial estimates for σ_G^2 and σ_B^2 . In particular, two different measures of statistical dispersion [29] are used, namely, the mean absolute deviation (MNAD, \mathcal{M}_e) and the median absolute deviation (MDAD, \mathcal{M}_d). In the following, \mathcal{M}_e and \mathcal{M}_d are defined, and the relative advantages of each are discussed. It should be noted that simply computing the conditional expectation of the variance is not feasible here because the overall distribution is a mixture of univariate Gaussians, and thus the expectation would be prone to errors resulting from outliers for each component Gaussian distribution.

Mean absolute deviation: The mean absolute deviation \mathcal{M}_e for a sample $\mathcal{X} = \{X_1, \dots, X_N\}$ of a random variable X is defined as

$$\mathcal{M}_e(\mathcal{X}) = \frac{\sum_{i=1}^N |X_i - \text{mean}(\mathcal{X})|}{N}. \quad (9)$$

Since the computation of \mathcal{M}_e involves only summation and averages, the overall complexity of the estimation algorithm (and effectively of the receiver) increases only incrementally. Initial estimates are then obtained by setting $\mathcal{T}_{\text{blind}} = \mathcal{M}_e$ as the threshold for declaring outliers. One caveat that needs to be noted here is that although inordinately simple to compute, \mathcal{M}_e requires double averaging, and hence the quality of estimates using \mathcal{M}_e is susceptible to the variations in P_B (for comparable SIR levels) and therefore also to sample size. An improved approach that is more robust to such variations is presented next.

Median absolute deviation: The median absolute deviation \mathcal{M}_d is considered to be a robust parameter in the presence of statistically deviant observations [29], and the motivation stems partly from the fact that MDAD is similar to rank-based non-parametric tests (for example,

the Wilcoxon detector [26, pp. 117–118]) that are typically considered to be robust statistical tests. The median of the received block of symbols is used to compute a threshold (\mathcal{M}_d) that is robust to the Markov chain probabilities governing the evolution of the noise process. The MDAD is computed as

$$\mathcal{M}_d(\mathcal{X}) = \sum_{i=1}^N |X_i - \text{median}(\mathcal{X})|. \quad (10)$$

The threshold $\mathcal{T}_{\text{blind}} = \mathcal{M}_d$ is applied to identify outliers in this case. While the MDAD is in general more robust than the MNAD, it should be noted that there is an additional complexity of computing the median of the received samples.

For both MNAD and MDAD, the estimation proceeds similarly to the semi-blind case, and (8) is again employed to obtain $\hat{\sigma}_B^2$ from the set \mathcal{O} , where the elements of \mathcal{O} are now obtained using $\mathcal{T}_{\text{blind}}$, as computed in (9) and (10). Furthermore, an initial estimate for σ_G^2 is also obtained by using $y_k \in \mathcal{O}$ in (8). However, for the computation of the σ_G^2 equal weighting factors, $\eta_k = |\mathcal{O}|^{-1}$ is used, which effectively results in an estimate equal to the conditional mean of \mathcal{O} . Statistically, this is prudent, since under the assumption that \mathcal{O} contains only non-interfered samples, the mean is the best unbiased estimator for univariate noise [26]. It is obvious that the unique advantage of the blind methods is that prior information regarding the parameters of the noise process is not a prerequisite for estimating the statistics of the interfering signals.

IV Conventional and genie-aided detector

The JSS approach is expected to afford a higher instantaneous IT and thus create greater opportunities for cognitive radios to transmit. To put its performance into context, two other receiver schemes are considered for comparison. The first is an idealized detector, for which it is assumed that a genie informs the primary user's receiver of the interference state and parameters at each time epoch. Then the receiver would apply the decoding metric

$$\lambda(\tilde{x}_k | s_k) = \frac{-|y_k - \sqrt{E_s}\tilde{x}_k|^2}{\sigma_{s_k}^2}. \quad (11)$$

A receiver using this metric is referred to as a genie-aided detector (GAD). While this is an unrealizable idealization, it is the best that one can do (given a code) and hence constitutes a yardstick for measuring the performance of the JSS algorithms.

A conventional primary user that does not employ its channel sensing abilities for noise state estimation or in general fails to account for signal degradation due to potential interferers assumes only AWGN at the receiver and applies the classical Euclidean-distance metric

$$\lambda(\tilde{x}_k) = -|y_k - \sqrt{E_s}\tilde{x}_k|^2, \quad (12)$$

which is mismatched in the presence of interference and hence can be expected to have relatively poor performance for the scenarios considered here. This detector is referred to as a Gaussian-noise detector (GND) in the following.

V Results and discussion

The results of the performance evaluations of the proposed semi-blind and blind estimation approaches are now presented through Monte Carlo simulations. A maximum free-distance, rate-1/2, memory-4 convolutional encoder with generator polynomials (23)₈ and (35)₈ is employed. The average duration of an interference burst is considered to be $\bar{T}_B = 40$ symbols for all results presented, and a value of $N = 5000$ is considered for simulative purposes. All other relevant parameters of the noise process can be determined from P_B and

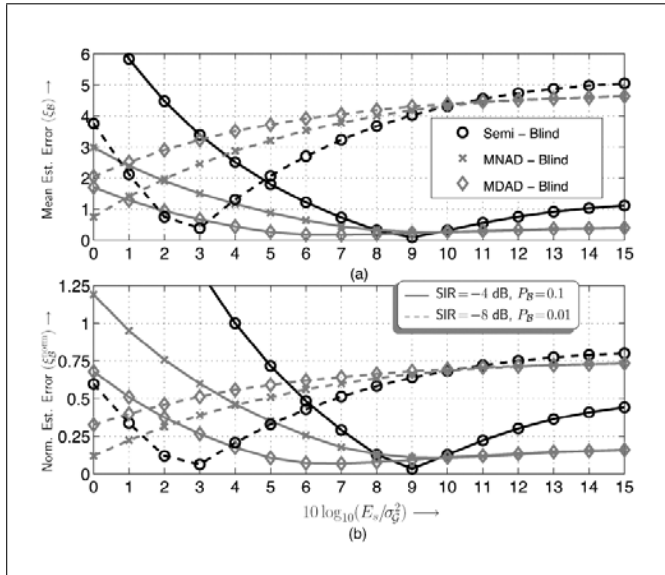


Figure 3: Estimation error for noise variance in the bad state, σ_B^2 , when semi-blind and blind JSS approaches are employed: (a) MEE and (b) normalized MEE for $P_B = 0.1$, SIR = -4 dB (dashed lines) and $P_B = 0.01$, SIR = -8 dB (solid lines). Estimation error can be seen to be limited to within an order of magnitude for the SNR values of interest.

\bar{T}_B [30]. BER is used as a target performance criterion, and BER equal to 10^{-4} is set to be the maximum allowable error rate at a primary receiver when secondary users are active. The factors that affect the BER at a given SNR are the probability of interference, P_B , and the SIR levels at the primary receiver. The underlying assumption with an interference temperature-based cognitive transmission environment is that secondary users will be allowed to transmit as long as $\sigma_G^2 + \sigma_B^2$ is less than a certain IT threshold. However, since the interference occurs with a probability P_B , it plays a defining role in determining what threshold levels are allowed. To highlight this point, a value of $P_B = [0.1, 0.01]$, representing two different rates of occurrence for interfering signals, is considered. It was found that, given a BER upper limit of 10^{-4} , the minimum allowable SIR for GND with $P_B = 0.1$ is -4 dB, and with $P_B = 0.01$ is -8 dB, when no measures for interference mitigation are adopted, i.e., GND is used. The SIR values corresponding to the two interference scenarios will be referred to as *sustainable* SIRs for the respective P_B values. For evaluative purposes, in the following the parameterizations with $[P_B = 0.1, \text{SIR} = -4 \text{ dB}]$ and $[P_B = 0.01, \text{SIR} = -8 \text{ dB}]$ are denoted as Case I and Case II respectively.

V.A Estimation error

A classical performance metric for any statistical estimation technique is the error in estimating the quantities of interests. For the present case, the two relevant quantities are (a) the variance of the noise at each epoch and (b) the noise state itself. The variance estimation error for the blind and semi-blind estimation techniques is quantified in terms of the mean estimation error (MEE) $\xi_S = E[|\sigma_S^2 - \hat{\sigma}_S^2|]$ and the normalized mean estimation error $\xi_S^{\text{norm}} = \xi_S/\sigma_S^2$, which is indicative of the order-of-magnitude error in the estimation process. Figs. 3(a) and 3(b) depict ξ_B and ξ_B^{norm} respectively for the initial estimates obtained by applying (8). Results for both Case I (solid lines) and Case II (dashed lines) are presented in order to highlight the effect of P_B and the strength of the interfering signals on the respective performances of MNAD and MDAD. Asymptotically, it can be observed that a lower P_B will lead to larger errors in estimation of σ_B^2 as the sample size for \mathcal{O} is smaller. The opposite will be seen to hold true for the estimation of σ_G^2 (see Fig. 4) as the corresponding sample size is larger with lower P_B . Also, it should be noted that because of the way the threshold is defined for the semi-blind algorithm, its error curves exhibit an inflexion that is a consequence of its explicit dependence on σ_G^2 , whereas the curves for blind methods are monotonic. Furthermore, it is encour-

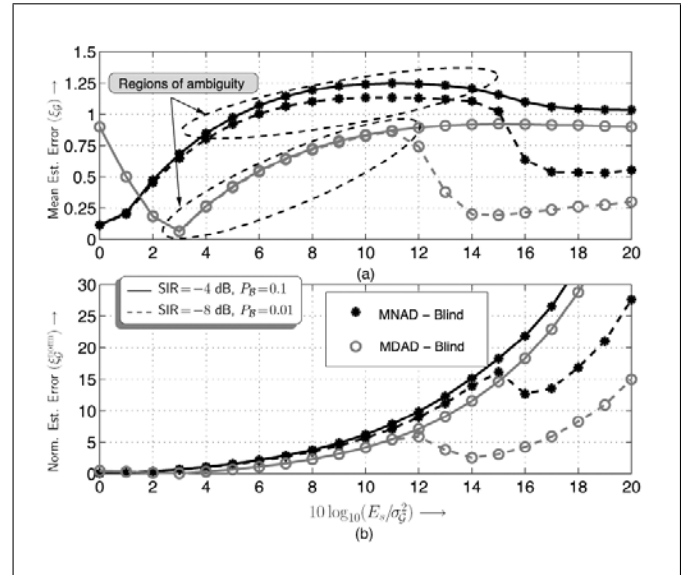


Figure 4: Estimation error for noise variance in the good state, σ_G^2 , when blind estimation techniques from Section III.C.2 are employed: (a) MEE and (b) normalized MEE for $P_B = 0.1$, SIR = -4 dB and $P_B = 0.01$, SIR = -8 dB respectively. The absolute error in estimation is fairly small compared to σ_B^2 , although normalized MEE may be several times higher.

aging to note that for SNR values of interest, ξ_B^{norm} is less than or equal to 1 for almost all detectors, i.e., the error is less than an order of magnitude. The results of Fig. 3 also indicate that regardless of the interference scenario, asymptotically both blind methods perform similarly, implying similar bootstrap values for σ_B^2 at these SNR values. Since the estimation algorithm is initially uninformed with respect to the Markovianity of the overall noise, one can expect that the key performance differentiator at high SNR will be the estimation of σ_G^2 , as will be discussed next.

Fig. 4 provides the corresponding estimation error results for σ_G^2 when blind estimation is employed. Different from the results for σ_B^2 , although the ξ_G values are fairly nominal, the values for ξ_G^{norm} reveal that in general $\hat{\sigma}_G^2$ is several times higher than σ_G^2 for moderate-to-high values of SNR. This result can be explained intuitively by taking a closer look at the role of E_s in the expression for initial estimate in (8). It is apparent that E_s , regardless of the transmitted symbol, will play a key role in determining $\hat{\sigma}_G^2$. While this fact is not an issue for low-to-moderate SNRs, it puts a limit on the accuracy of the estimation of σ_G^2 at high SNR values as σ_G^2 is several orders lower than E_s . For example, at SNR = 12 dB, σ_G^2 is roughly 16 times lower than E_s . This explains the higher ξ_G^{norm} for higher SNR values and the corresponding flatness in ξ_G . Interestingly, far more variations are seen in the slope of the MEE curves for σ_G^2 than for σ_B^2 . This behaviour of ξ_G can be attributed to the existence of regions of ambiguity in determining the membership of a received symbol in \mathcal{O} . For SNR ranges where $E_s + \sigma_G^2$ is comparable to σ_B^2 , the ability of the decision device to discern whether the energy contained in the received symbol is attributed primarily to the transmitted signal, the white Gaussian noise, or the interference signal is impaired and may result in erroneous classification of a received symbol. These ambiguities manifest themselves to a much lesser extent in the estimation of σ_B^2 since $\sigma_B^2/\sigma_G^2 \gg 1$ for most reasonable values of channel SNR, implying that, contrary to $\hat{\sigma}_G^2$, added contributions from E_s or σ_G^2 cause only minor changes in the value of $\hat{\sigma}_B^2$. It should be further noted that in terms of impact on BER, the need to make this distinction is less critical at very low SNR values where σ_G^2 itself is high, and consequently so are the receiver error rates. Moreover, it is easy to see that such distinctions are relatively easier to make for low SIR values and high SNR values. Results that further elaborate the impact of the regions of ambiguity on BER are presented in Section V.C.

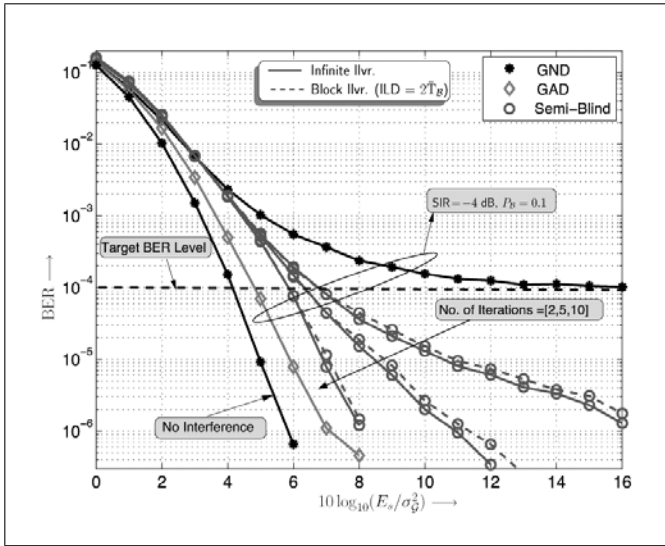


Figure 5: Bit error rates with semi-blind JSS for Case I parameters. Performance with 10 iterations closely approaches that of GAD, while GND floors at relatively higher BERs, needing a boost of about 10 dB in its operating SNR to meet the target BER levels.

The refinement in estimation of \mathbf{s} over iterations is now considered by evaluating the probability of false estimation (P_{FE}) of states for Cases I and II. Typically, the probability of a false alarm (P_{FA}) i.e., the probability of deciding that an interferer is present when there is none (asserting that \mathcal{H}_1 is true instead of \mathcal{H}_0) and the probability of missed detection (P_{MD}) (asserting \mathcal{H}_0 when \mathcal{H}_1 is true) are used to determine the efficiency of a statistical hypothesis test [26]. P_{FE} subsumes both these criteria by considering the case when \mathcal{H}_T is inferred when \mathcal{H}_F , $T \in \{0, 1\}$, is true, i.e., $P_{FE} = P_{FA} + P_{MD}$. Table 1 presents P_{FE} for semi-blind and blind JSS approaches in percentage form for up to 10 iterations at SNR = 8 dB. Semi-blind estimation can be seen to be highly effective as the number of wrongly estimated states is reduced to less than 1.0% for both cases with a maximum of 10 iterations. Also, in both interference scenarios, the rate of decay of P_{FE} with iterations is much faster for semi-blind JSS than for the blind methods. It is also observed that P_{FE} is in general several times lower for SIR = -8 dB than for SIR = -4 dB, corroborating the earlier assertion that lower SIR aids in reducing ambiguity in outlier rejection. The order of error observed for the blind techniques after the first iteration is comparable to the frequency of occurrence of the impulsive signal, i.e., P_B , which is seen to diminish gradually over iterations. The rather sluggish improvement in estimation for the blind method suggests that far more iterations compared to the semi-blind method will be required for substantial improvements in the BER. This inference guides the following consideration of the possible BER enhancements achievable through the proposed methods.

V.B Bit error rate

Bit error rate is a tangible measure of increments in the IT threshold that can be realized while meeting transmission-reliability constraints such as packet loss and maximum number of retransmissions. In this section, the BER results obtained when JSS is employed as described in Section III.A are presented, and the results are benchmarked with standard receivers (Section IV). Towards this end, Fig. 5 presents the performance curves for semi-blind JSS with 2, 5, and 10 iterations for Case I. Results are shown for both infinite and finite interleaving with $ILD = 2T_B$ to emphasize that practical interleavers that are designed to meet maximum-delay requirements are equally applicable. From the BER curves of GND for the case of no interference, i.e., with no other users being active, cognitive or otherwise, it can be seen that for a permitted SIR of -4 dB, an increase of roughly 10 dB in the operating SNR is required to meet the target BER level. The primary motivation in estimating the noise state and variance is the fact that perfect knowledge of these parameters (GAD curve) allows a reduction in the required increase in the operating SNR to about 1 dB, which is a huge

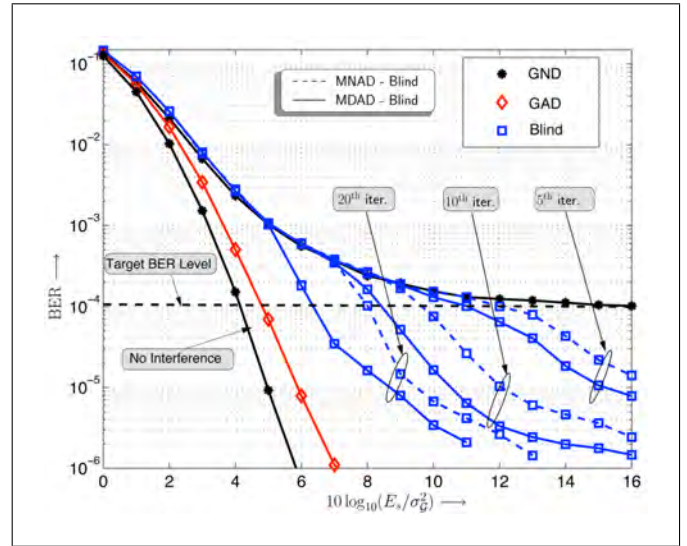


Figure 6: Performance comparison of the MNAD and MDAD blind JSS methods for Case I parameters. Substantial gains in operating SNR are observed after 10 iterations, a distinctly lower number than required by the semi-blind method. Performance gains similar to those of the semi-blind approach are seen to be achieved when twice the number of iterations required by the semi-blind approach are used.

Table 1
Percentage of falsely estimated states (P_{FE}) using the semi-blind and blind estimation algorithms at SNR $E_s/\sigma_g^2 = 8$ dB for Case I ($P_B = 0.1$, SIR = -4 dB) and Case II ($P_B = 0.01$, SIR = -8 dB)

Iter.	Semi-blind		MDAD-blind		MNAD-blind	
	Case I	Case II	Case I	Case II	Case I	Case II
2	14.2850	14.1126	9.9698	0.9187	12.6256	0.9011
4	7.0016	4.4046	9.9639	0.8676	12.3718	0.8535
6	3.6192	1.4834	9.6562	0.7348	10.1035	0.7248
8	1.4725	0.5832	8.9799	0.6898	9.9466	0.6283
10	0.6027	0.2514	8.1472	0.6304	9.8853	0.6177

improvement over the requirement for GND. To this end, it is encouraging to observe that semi-blind JSS can recover much of the damage done by the interfering signals and, although not ideal, it does offer reductions of about 7 dB in the operating SNR after only two iterations. Moreover, the error floor witnessed for the GND is practically eliminated through more iterations of the algorithm, such that performance after 10 iterations is seen to closely approach that of the GAD. In addition, the BER performance curves with finite interleaving are seen to be only slightly worse than those with infinite interleaving, implying minor degradations due to non-ideal interleaving. The improvements observed through the application of the semi-blind JSS algorithm serve as a classic example of a case where JSS can provide enormous gains. In particular, depending on the applicable path loss model [31], and assuming that SNR boosts of up to 10 dB (as in Fig. 5) can be accommodated by the primary transmission system, one can significantly reduce the region of interference of the primary user (refer to Fig. 2). This, in effect, implies that far more cognitive users may be allowed to be active, as they are no longer in the no-talk zone of the primary receiver.

Fig. 6 compares the performance of the blind approaches presented in Section III.C with the conventional approaches when applying infinite interleaving for the interference scenario of Case I. It can be seen that for both MNAD and MDAD blind estimation, the gains for up to 10 iterations are relatively lower compared to the semi-blind technique. In general, MDAD-blind performs better than MNAD-blind for

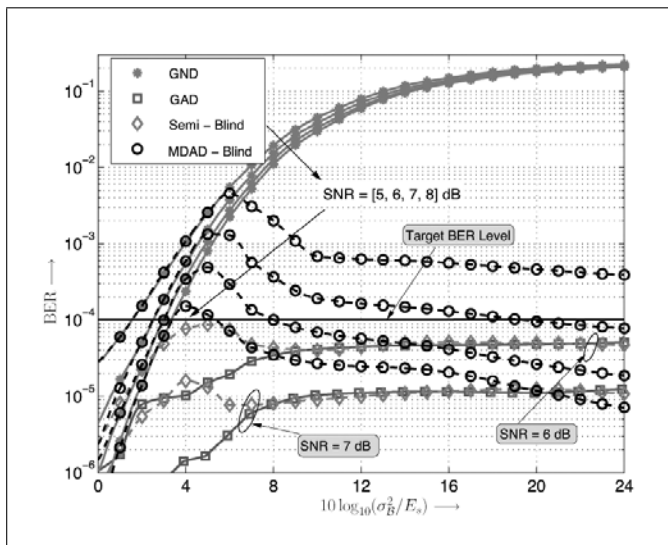


Figure 7: Interference tolerance of the various detectors depicted in terms of achievable BER with decreasing SIR when P_B is held constant at 0.1 and target BER is equal to 10^{-4} . Beyond a certain region of ambiguity, which is SNR-dependent, target BER levels are seen to be easily achieved within 10 iterations for the JSS algorithms with only minor increases in the link budget of the primary user.

the considered P_B and SIR values. The gain in terms of required SNR reduction after 10 iterations is limited to roughly 4 dB and 6 dB for MNAD-blind and MDAD-blind respectively. Nonetheless, these gains are large enough to allow for reduced link budgets and/or reduced regions of interference for the primary receiver. Fig. 6 also shows that if the primary receiver has the requisite processing power and is not limited by delay constraints, 20 iterations of the blind JSS algorithms can improve performance further by roughly 2 dB for both MNAD and MDAD. Admittedly, the blind approaches are less effective than the semi-blind approach in terms of lowering the error floor of the system, but they are an order of magnitude or more lower than the GND. Although not shown here because of space constraints, similar performance patterns were observed for Case II, with MDAD performing visibly better than the MNAD approach.

V.C Benefits of JSS in a cognitive environment

In this section, the benefits derived from the application of the JSS algorithm at receivers in a multi-user cognitive environment, pertaining to both primary and secondary users, are briefly discussed.

V.C.1 Increased interference tolerance

The BER results for the proposed receiver structures in Figs. 5 and 6 suggest that there are distinctive gains associated with the interference state and variance estimation as proposed in this paper. Therefore, it is interesting to discern what levels of interference can be tolerated at the receiver, i.e., how large σ_B^2 may be such that nominal increases in the link budget can help meet the target BER requirement of 10^{-4} . To this end, Fig. 7 presents the BERs of various detectors (except MNAD-blind) as a function of decreasing SIR with the probability of interference held constant at $P_B = 0.1$. For the GND and the MDAD-blind detectors, results are presented for SNR = [5, 6, 7, 8] dB, while for semi-blind JSS and GAD, results are presented only for SNR = [6, 7] dB, as these values of SNR are seen to be sufficient to attain BER values lower than 10^{-4} over the entire range of SIR values considered. Several insightful observations can be made here that help to provide an appreciation of the capabilities of the proposed algorithms. First, it can be seen that the conventional GND is ill-equipped to handle interference levels beyond SIR = -4 dB with nominal increases in the SNR. In fact, in Fig. 6 it was observed that even for substantially high SNR values, the GND runs into an error floor in the presence of interference. By contrast, for JSS-based receivers it can be seen that effective mitigation of fairly high levels of

interference is possible by increasing the operating SNR by a few decibels over and above the no-interference level, i.e., 4 dB (see Fig. 6). However, for SIR values at which the desired signal energy and interference signal energy are comparable, it is seen that the region of ambiguity is in play because discriminating between primary signal and interference solely on the basis of received energy is challenging. Also, semi-blind JSS is seen to closely mimic the performance of the GAD beyond a certain threshold SNR. Overall, Fig. 7 indicates that effective interference mitigation can allow the primary receiver to maintain its quality-of-service levels while accommodating several unlicensed users.

V.C.2 Advantages to secondary user

While most of the discussion in this paper has centred around the primary user, JSS can also be applied at the secondary receiver to provide greater protection against other cognitive users (say, T_s^2 in Fig. 2) that will play the role of co-channel interferers. In real-world transceivers, filters are never ideal, and noise is neither Gaussian nor white [4]. Thus one can hardly guarantee complete immunity from impulsive interference to secondary users when they are allowed to transmit. Implementing a JSS-based receiver is easier at the CR transceiver since it has built-in sensing abilities by definition. Moreover, JSS can also reduce link budgets for secondary users and consequently the perceived IT levels at the primary user, which is the primary goal.

VI Concluding remarks

In this paper a design paradigm was provided for throughput enhancement in a cognitive radio environment, using a receiver-centric approach to interference mitigation and allowing for a reduction in the region of interference of the primary user. The non-Gaussian nature of the interference is exploited in a way that permits the receivers to have a much higher instantaneous IT threshold than permitted by conventional receiver structures. In particular, a joint sensing and suppression algorithm was presented that allows a primary user to communicate with a low probability of error even when there are potentially harmful interfering signals. Semi-blind and blind approaches to estimation of the interference process were presented with the interference modelled as a first-order Markovian process. Both approaches were shown to offer significant enhancements in interference mitigation, with the semi-blind method exhibiting only minor degradation with respect to a hypothesized ideal receiver. The benefits derived were in the form of a potentially higher spectrum utilization and increased protection from ambient interfering signals.

Acknowledgements

The authors would like to thank Prof. Matías Salibián-Barrera (Department of Statistics, University of British Columbia) for suggesting the use of the median absolute deviation for blind estimation.

References

- [1] Federal Communications Commission (FCC), "Spectrum policy task force," FCC, Tech. Rep. ET Docket No. 02-135, Nov. 2002.
- [2] A. Petrin and P.G. Steffes, "Measurement and analysis of urban spectrum usage," in *Proc. Int. Symp. Advanced Radio Technologies (ISART)*, Boulder, Colo., July 27-30, 2004.
- [3] S. Haykin, "Cognitive radio: Brain-empowered wireless communication," *IEEE J. Select. Areas Commun.*, vol. 23, no. 2, Feb. 2005, pp. 201-220.
- [4] R. Tandra and A. Sahai, "SNR walls for signal detection," *IEEE J. Select. Topics Signal Processing*, vol. 2, no. 1, Feb. 2008, pp. 4-17.
- [5] E. Adamopoulou, K. Demestichas, and M. Theologou, "Enhanced estimation of configuration capabilities of cognitive radio," *IEEE Commun. Mag.*, vol. 46, no. 4, Apr. 2008, pp. 56-63.

- [6] J. Bater, H.-P. Tan, K.N. Brown, and L. Doyle, "Modeling interference temperature constraints for spectrum access in cognitive radio networks," in *Proc. IEEE Int. Conf. Commun.*, 2007, pp. 6493–6498.
- [7] X. Hong, C.-X. Wang, and J. Thompson, "Interference modeling of cognitive radio networks," in *Proc. IEEE Veh. Technol. Conf.*, May 2008, pp. 1851–1855.
- [8] N. Devroye, P. Mitran, and V. Tarokh, "Achievable rates in cognitive radio channels," *IEEE Trans. Inform. Theory*, vol. 52, no. 5, May 2006, pp. 1813–1827.
- [9] A. Somekh-Baruch, S. Shamai, and S. Verdú, "Cognitive interference channels with state information," in *Proc. Int. Symp. Information Theory (ISIT)*, July 2008, pp. 1353–1357.
- [10] D. Cabric, S.M. Mishra, and R.W. Brodersen, "Implementation issues in spectrum sensing for cognitive radios," in *Proc. 38th Asilomar Conf.*, 2004, pp. 772–776.
- [11] D. Cabric and R.W. Brodersen, "Physical layer design issues unique to cognitive radio systems," in *Proc. Personal, Indoor and Mobile Radio Communications Symp. (PIMRC 2005)*, 2005, pp. 759–763.
- [12] R. Tandra, S.M. Mishra, and A. Sahai, "What is a spectrum hole and what does it take to recognize one?" *Proc. IEEE*, vol. 97, no. 5, May 2009, pp. 824–848.
- [13] P.C. Pinto and M.Z. Win, "Communication in a Poisson field of interferers," in *Proc. Conf. Inform. Sci. Syst. (CISS)*, Mar. 2006, pp. 432–437.
- [14] S. Kassam, *Signal Detection in Non-Gaussian Noise*, Berlin: Springer Verlag, 1988.
- [15] N.C. Beaulieu and A.A. Abu-Dayya, "Bandwidth efficient QPSK in cochannel interference and fading," *IEEE Trans. Commun.*, vol. 43, no. 9, Sept. 1995, pp. 2464–2474.
- [16] M. Ghosh, "Analysis of the effect of impulse noise on multicarrier and single carrier QAM systems," *IEEE Trans. Commun.*, vol. 44, no. 2, Feb. 1996, pp. 145–147.
- [17] X. Yang and A.P. Petropulu, "Co-channel interference modeling and analysis in a Poisson field of interferers in wireless communications," *IEEE Trans. Signal Processing*, vol. 51, Jan. 2003, pp. 64–76.
- [18] J.-W. Moon, T.F. Wong, and J.M. Shea, "Pilot-assisted and blind joint data detection and channel estimation in partial-time jamming," *IEEE Trans. Commun.*, vol. 54, no. 11, Nov. 2006, pp. 2092–2102.
- [19] R.J. Zozick, R.S. Blum, and B.M. Sadler, "Signal processing in non-Gaussian noise using mixture distributions and the EM algorithm," in *Proc. Asilomar Conf.*, Nov. 1997, pp. 438–442.
- [20] J. Mitra and L. Lampe, "On joint estimation and decoding for channels with noise memory," *IEEE Commun. Lett.*, vol. 13, no. 10, Oct. 2009, pp. 730–732.
- [21] G. Colavolpe, G. Ferrari, and R. Raheli, "Extrinsic information in iterative decoding: A unified view," *IEEE Trans. Commun.*, vol. 49, Dec. 2001, pp. 2088–2094.
- [22] L.R. Bahl, J. Cocke, F. Jelinek, and J. Raviv, "Optimal decoding of linear codes for minimizing symbol error rate," *IEEE Trans. Inform. Theory*, vol. 20, no. 2, Mar. 1974, pp. 284–287.
- [23] D.R. Pauluzzi and N.C. Beaulieu, "A comparison of SNR estimation techniques for the AWGN channel," *IEEE Trans. Commun.*, vol. 48, Oct. 2000, pp. 1681–1691.
- [24] R. Menon, R.M. Buehrer, and J.H. Reed, "Outage probability based comparison of underlay and overlay spectrum sharing techniques," in *Proc. 1st IEEE Int. Symp. New Frontiers in Dynamic Spectrum Access Networks (DySPAN 2005)*, Baltimore, Md., Nov. 2005, pp. 101–109.
- [25] J. Bilmes, "A gentle tutorial on the EM algorithm and its application to parameter estimation for Gaussian mixture and hidden Markov models," Berkeley, Calif., International Computer Science Institute, Tech. Rep. TR-97-021, 1997.
- [26] H.V. Poor, *An Introduction to Signal Detection and Estimation*, 2nd ed., New York: Springer Verlag, 1994.
- [27] A. Sahai, R. Tandra, S. Mishra, and N. Hoven, "Fundamental design tradeoffs in cognitive radio systems," in *Proc. 1st Int. Workshop on Technology and Policy for Accessing Spectrum (TAPAS)*, 2006.
- [28] P. Huber, *Robust Statistics*, New York: John Wiley & Sons, Inc., 1981.
- [29] E. Jondeau, S.-H. Poon, and M. Rockinger, *Financial Modeling under Non-Gaussian Distributions*, London: Springer, 2007.
- [30] M. Mushkin and I. Bar-David, "Capacity and coding for Gilbert-Elliott channels," *IEEE Trans. Inform. Theory*, vol. 35, Nov. 1989, pp. 1277–1290.
- [31] T.S. Rappaport, *Wireless Communications: Principles and Practice*, 2nd ed., Singapore: Pearson Education, 2002.



Jeebak Mitra (S'03) received a B.Eng. degree in electronics and communication engineering from Birla Institute of Technology, Ranchi, India, in 2002 and an M.A.Sc. in electrical engineering from the University of British Columbia (UBC), Vancouver, British Columbia, Canada, in 2005. From July 2002 to July 2003 he worked as an Expert Team member in the Contact Center Solutions Group of AVAYA GlobalConnect (Tata Telecom) India. He is currently a Ph.D. candidate and research assistant with the Communication Theory Group at UBC. He received the Best Student Paper Award in 2009 at the IEEE Canadian Conference on Electrical and Computer Engineering (CCECE) and won second place in the Ind-US Entrepreneurs (TiE) National Paper Presentation Competition in 2002. He also received the International Partial Tuition Scholarship and the Ph.D. Tuition Award from UBC in 2003 and 2006 respectively. His research interests lie broadly in the area of physical-layer communication for both wireless and wireline networks with an emphasis on design and analysis of receivers in interference-limited environments. He also serves regularly as a reviewer for several conferences and journals in related areas.



Lutz Lampe (M'02-SM'08) received the Diplom (Univ.) and Ph.D. degrees in electrical engineering from the University of Erlangen, Germany, in 1998 and 2002, respectively. Since 2003 he has been with the Department of Electrical and Computer Engineering at the University of British Columbia, Vancouver, British Columbia, Canada, where he is currently an associate professor. He is a co-recipient of the *Eurasip Signal Processing Journal* Best Paper Award 2005 and the Best Paper Award at the 2006 IEEE International Conference on Ultra-Wideband. In 2003, he received the Dissertation Award of the German Society of Information Techniques. He was awarded the UBC Killam Research Prize in 2008 and the Friedrich Wilhelm Bessel Research Award by the Alexander von Humboldt Foundation in 2009. He is an editor for the *IEEE Transactions on Wireless Communications* and the *International Journal on Electronics and Communications* (AEUE), and he served as associate editor for the *IEEE Transactions on Vehicular Technology* from 2004 to 2008. He is vice-chair of the IEEE Communications Society Technical Committee on Power Line Communications. He was general chair of the 2005 International Symposium on Power Line Communications and the 2009 IEEE International Conference on Ultra-Wideband. He is co-editor of the comprehensive book *Power Line Communications* (Wiley).